Astron. Astrophys. 263, 423–432 (1992)

ASTRONOMY AND ASTROPHYSICS

Optical properties of dust aggregates

I. Wavelength dependence

Takashi Kozasa[1*] **, Jürgen Blum**[1]**, and Tadashi Mukai**[2]

[1] Max–Planck–Institut für Kernphysik, W–6900 Heidelberg 1, Federal Republic of Germany
[2] Department of Earth Sciences, Kobe University, Kobe 657, Japan

Received February 22, accepted May 16, 1992

Abstract. Optical properties of dust aggregates of astrophysical interest have been investigated by means of the discrete dipole approximation (DDA) to clarify how differences in structure, size and chemical composition of dust aggregates affect their optical properties. Two types of dust aggregates have been treated; one is the Ballistic Particle–Cluster Aggregates (BPCA) whose fractal dimension $D \sim 3$, and the other is the Ballistic Cluster–Cluster Aggregates (BCCA) for which $D \sim 2$. Two kinds of minerals have been considered for the constituent particles; silicate and magnetite.

The results of the calculations show that the optical properties of dust aggregates are divided into two regimes according to their characteristic size a_c; in the wavelength range $\lambda \gg \lambda_c = 2\pi a_c$, the optical properties are qualitatively reproduced by the Rayleigh approximation for a sphere with the same mass and do not depend on the structure of the dust aggregates. The scattering cross sections start to deviate from the Rayleigh regime at about the characteristic wavelength $\lambda_c = 2\pi a_c$, which is a diagnostic for the sizes of dust aggregates, irrespective of the chemical composition of the constituent particles.

The wavelength dependence of the absorption cross sections can be interpreted in terms of the optical thickness of the dust aggregates themselves and can be approximated with a simple formula. This formula is useful to determine the dependence of the temperature of dust aggregates in space on their sizes as well as structures, which plays a crucial role in considering the physical and chemical evolution of dust aggregates in space.

The wavelength dependence of the asymmetry parameter reflects the size as well as the structure of dust aggregates, independent of the chemical composition of the constituent particles. BPCA are characterized by an enhanced forward scattering in the region of $\lambda \ll \lambda_c$ in comparison with BCCA with the same mass, in spite of the smaller size of BPCA.

The applicability of the Maxwell–Garnett mixing rule to dust aggregates is investigated in comparison with the results of the calculations using the discrete dipole approximation.

Key words: optical properties – dust aggregates – fractals – interstellar/interplanetary dust

Send offprint requests to: Jürgen Blum
* The Institute of Space and Astronautical Science, Sagamihara, Kanagawa 229, Japan

1. Introduction

Dust aggregates exist in a variety of astrophysical environments; cometary atmospheres (Greenberg & Hage 1990), interplanetary space (Brownlee et al. 1976; Giese et al. 1978), and molecular clouds (Mathis 1990; references therein). Also Mathis & Whiffen (1989) have claimed that interstellar dust seems to be dust aggregates composed of several kinds of astrophysical minerals whose radii are ~ 50 Å.

The optical properties of dust aggregates play a crucial role in considering many astrophysical problems related to dust grains; physical and chemical evolution of dust in space, thermal balance in molecular clouds, dynamical behavior of dust due to radiation pressure forces, and deduction of the structure, the size, and the chemical composition of dust particles in space by comparison with observations as well as with laboratory experiments.

Many authors have tried to calculate the optical properties of dust particles with irregular shapes and/or fluffy structures by means of a variety of methods: the effective medium theories (Jones 1989; Mathis & Whiffen 1989; Ossenkopf 1991), the RC network method (Wright 1987), the geometric ray tracing method (Muinonen et al. 1989), the discrete dipole approximation (Purcell & Pennypacker 1973; Draine 1988; Perrin & Lamy 1990; Perrin & Sivan 1990,1991), and the volume integration formulation (Hage & Greenberg 1990). On the other hand, the effects of structure and size of dust aggregates, and of the chemical composition of the constituent particles on their optical properties have not been studied systematically. Also very little is known about what types of structure dust aggregates have in space, although the cluster–cluster aggregates, which have very fluffy structures, are considered as representatives. (Wright 1987; Bazell & Dwek 1990).

Recently Blum and Kozasa (1992) have produced a variety of aggregates relevant to dust aggregates in space by 3–dimensional Monte–Carlo simulations. The results show that the structures of the dust aggregates heavily depend on their formation process, and that the dust aggregates must be characterized not only by their fractal dimension, but also by their mean porosity. On the basis of the results of these simulations, we investigate in this paper the optical properties of dust aggregates by means of the discrete dipole approximation (DDA), by replacing each constituent particle by a dipole. The reason why we replace the constituent particles by dipoles is to avoid some artificial

errors caused by dividing a constituent sphere into cubic cells, as demonstrated by Draine (1988).

Our goal is to clarify how the optical properties depend on the structure and the size of the dust aggregates, and on the chemical composition of the constituent particles. We treat two extreme types of dust aggregates whose number of constituent particles are 256, 512 and 1024, respectively. Also we consider two kinds of minerals for the constituent particle; silicate as an example of dielectric material and magnetite as an absorbing material. The emphasis is put on the wavelength dependence of the cross sections of light interaction with dust aggregates. In Sect. 2 the dust aggregates used for the calculations, and the method of the discrete dipole approximation are described. The results of the calculations are presented and discussed in Sect. 3. In Sect. 4, the wavelength dependence of the absorption cross sections is discussed in connection with the optical thickness of dust aggregates and also the applicability of the Maxwell–Garnett mixing rule to dust aggregates is investigated in comparison with the results of the calculations using the discrete dipole method. The concluding remarks are presented in Sect. 5.

2. Models of dust aggregates and the discrete dipole approximation

2.1. Models of dust aggregates

The dust aggregates have been produced by shooting projectiles onto a target randomly one at a time. The trajectories of the projectiles are assumed to be ballistic. In the simulation we consider that the projectiles are attached with a sticking probability to the target at the place where they hit the target. (see Blum & Kozasa 1992 for the details of the simulation and the results). In this paper we consider two extreme types of dust aggregates; one is the Ballistic Particle–Cluster Aggregates (BPCA) and the other is the Ballistic Cluster–Cluster Aggregates (BCCA). For BPCA the projectile is a constituent particle, while for BCCA the projectile is a dust aggregate which has the same mass as but different structure from the target. In both cases, the radii of the constituent particles are constant, and the sticking probability is 1. Figures 1a and 1b show both dust aggregates used for the calculations of the optical properties.

The structure of dust aggregates is usually represented in terms of the fractal dimension D, which is determined from the relation $N \propto R_g^D$, where N is the number of constituent particles and R_g is the radius of gyration of the dust aggregates. The fractal dimension is well defined for dust aggregates with $N \gtrsim 256$. The fractal dimensions are ~ 3 for BPCA and ~ 2 for BCCA in the limit of large sizes. From Figs. 1a and 1b, we can see that BCCA are larger in size and more fluffy in structure than BPCA with the same number of constituent particles, according to their fractal dimensions.

However, it should be noted that dust aggregates are not only characterized by their fractal dimensions. The results of the simulations have shown that the porosity is also an independent parameter to characterize dust aggregates, closely related with the formation process. Before the evaluation of the mean porosity, the characteristic radius a_c of the dust aggregate is defined in a manner consistent with the definition of the fractal dimension by $a_c = \sqrt{5/3}R_g$. The so defined characteristic radius represents the radius of a homogeneous sphere with a radius of gyration R_g, and the sphere in fact almost encloses the dust aggregate. The characteristic radius a_c, therefore, is considered to be the most plausible size to evaluate the volume–mean quantities of the dust aggregate. The mean porosity is calculated by $P = 1 - N(a_0/a_c)^3$, where a_0 is the radius of the constituent particle.

Table 1. The quantities that characterize the dust aggregates used for the calculations; the number of the constituent particles N, the characteristic radius a_c, the surface area–equivalent radius a_s, the mass–equivalent radius a_m, and the porosity P. Note that the radii of the constituent particles are 0.01 μm

Ballistic Particle–Cluster Aggregates (BPCA)				
N	a_c (μm)	a_s (μm)	a_m (μm)	P
256	0.1251	0.1103	0.0635	0.8694
512	0.1506	0.1408	0.0800	0.8501
1024	0.1904	0.1841	0.1008	0.8517
Ballistic Cluster–Cluster Aggregates (BCCA)				
N	a_c (μm)	a_s (μm)	a_m (μm)	P
256	0.2049	0.1241	0.0635	0.9703
512	0.4244	0.1741	0.0800	0.9933
1024	0.5320	0.2340	0.1008	0.9932

The geometric cross section A is also an important quantity that controls the surface phenomenae such as the interaction of light with the dust aggregate. The surface area–equivalent radius is evaluated by $a_s = \sqrt{A/\pi}$, and the geometric cross section A is the projected area averaged over three orthogonal directions. The mass–equivalent radius is $a_m = a_0 N^{1/3}$. These quantities that characterize the dust aggregates used in the calculation of the optical properties are summarized in Table 1, where the radii of the constituent particles are 0.01 μm.

2.2. The discrete dipole approximation

The discrete dipole approximation (DDA) has been applied to obtain the optical properties of an irregularly shaped and compact dust particle by dividing the body into unit cubic cells located on a cubic lattice (Purcell & Pennypacker 1973; Draine 1988). The size of a unit cell must be small enough to at least satisfy the condition $d/\lambda \ll 1$, where λ is the wavelength and d is the lattice spacing. Bazell & Dwek (1990) applied the discrete dipole method to a dust aggregate by dividing each constituent particle into cubic cells located on a cubic lattice. Their treatment is the basic method to treat dust aggregates consisting of constituent particles which do not satisfy the condition that the size parameter $x = 2\pi a_0/\lambda \ll 1$. However this method needs much memory to treat dust aggregates consisting of a large number of constituent particles. Also we should keep in mind that even if we divide a constituent spherical particle into unit cubic cells small enough to satisfy the above described condition, we cannot escape from some artificial enhancement of the light interaction cross sections stemming from the surface granularity as well as a lesser screening effect compared with a compact sphere, as demonstrated by Draine (1988).

We want to calculate the optical properties of dust aggregates whose constituent particles are not located on a cubic lattice. Also we want to reveal the effects of the process of aggregation itself on the optical properties of the dust aggregates. Therefore, in this paper we replace each constituent particle by a dipole and then

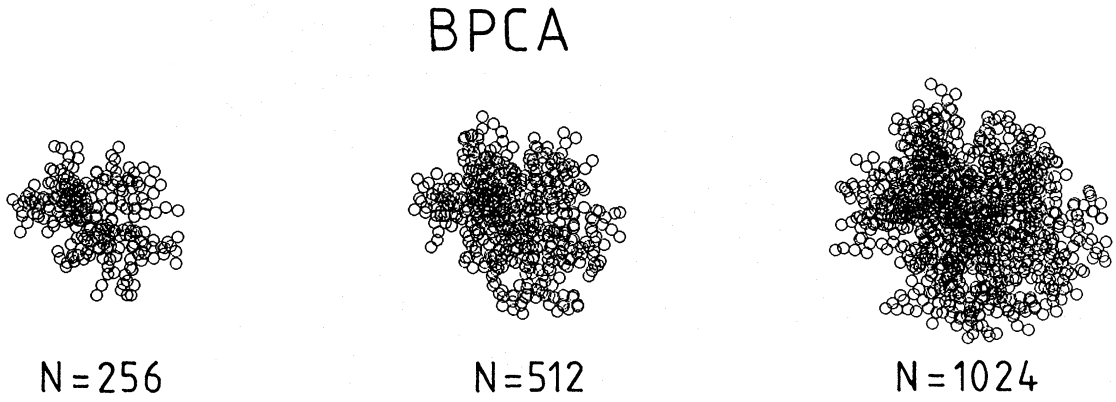

Fig. 1a. The Ballistic Particle–Cluster Aggregates (BPCA) used for the calculations, whose number of constituent particles are 256, 512, and 1024, respectively

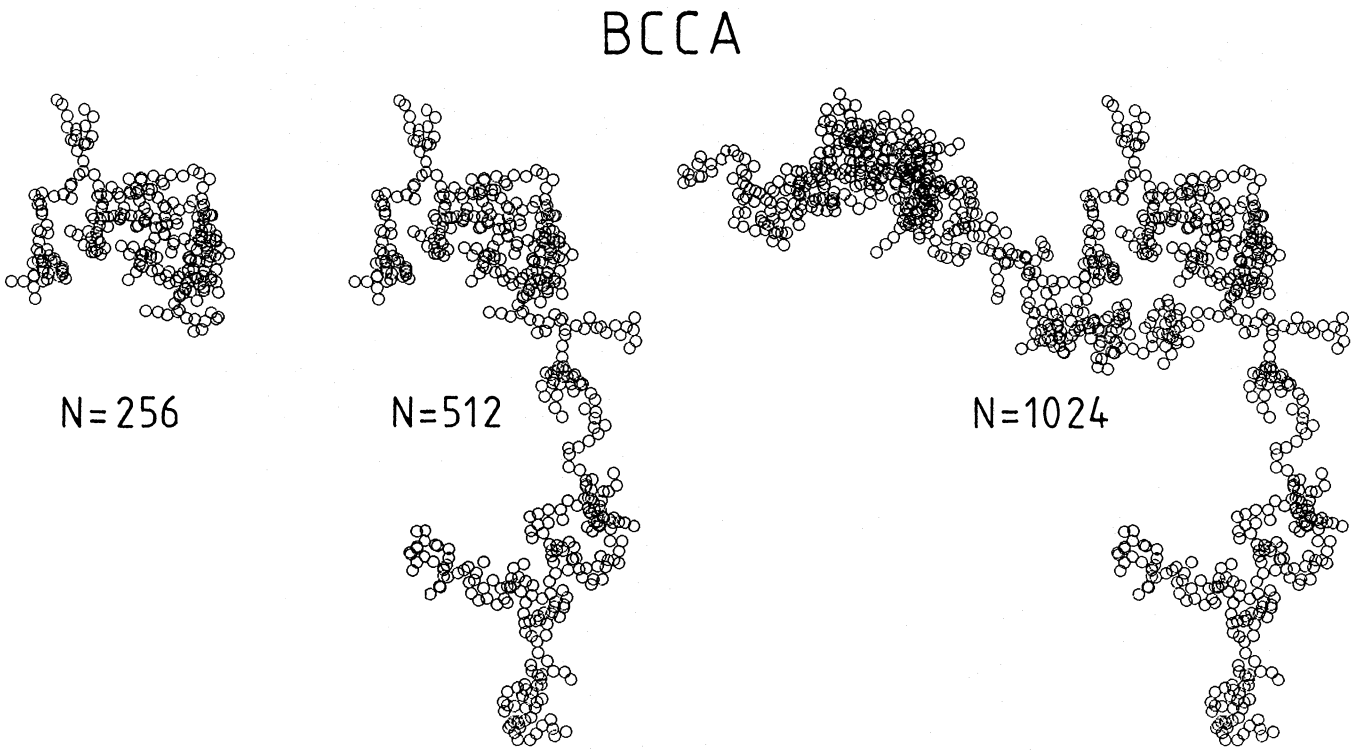

Fig. 1b. The same as Fig. 1a, but for the Ballistic Cluster–Cluster Aggregates (BCCA). The scale is the same as Fig. 1a. BCCA is larger in size and more fluffy in structure than BPCA

apply the discrete dipole method to the dust aggregates, though in this method the size of the constituent particles are limited small enough to at least satisfy the condition $x \ll 1$.

When each constituent sphere is replaced by a dipole, according to Hage & Greenberg (1990), we can formulate the discrete dipole method as follows: We consider the dust aggregate consisting of N homogeneous spheres with radii a_i and complex refractive indices m_i ($i = 1$ *to* N). Under the assumptions that the electric field inside the constituent particle is uniform, and that the interaction between different constituent particles is evaluated by the values at the center of the constituent particles, the electric field $\boldsymbol{E}(\boldsymbol{r}_i)$ (in cgs units) at the position of the i–th constituent particle is given by

$$\boldsymbol{E}(\boldsymbol{r}_i) = \boldsymbol{E}_0(\boldsymbol{r}_i) - \frac{m_i^2 - 1}{3}\boldsymbol{E}(\boldsymbol{r}_i) + \frac{2}{3}[(1 - ika_i)\exp(ika_i) - 1][m_i^2 - 1]\boldsymbol{E}(\boldsymbol{r}_i) + \frac{k^2}{3}\sum_{j\neq i}^{N}\mathbf{G}(\boldsymbol{r}_i, \boldsymbol{r}_j)[m_j^2 - 1]a_j^3\boldsymbol{E}(\boldsymbol{r}_j), \quad \text{for } i = 1 \text{ to } N, \tag{1}$$

where $\boldsymbol{r}_i$ is the position vector of the i–th constituent particle, and $\boldsymbol{E}_0(\boldsymbol{r}_i)$ is the incident electric field at $\boldsymbol{r}_i$. The Green function's dyadic is $\mathbf{G}(\boldsymbol{r}_i, \boldsymbol{r}_j)$ and the wave number $k = 2\pi/\lambda$. Note that the sign in Eq. (1) is different from Hage & Greenberg (1990), since we choose $e^{-i\omega t}$ as the form of the time variation of the electric field. The dipole moment $\boldsymbol{P}(\boldsymbol{r}_i) = (m_i^2 - 1)a_i^3\boldsymbol{E}(\boldsymbol{r}_i)/3$ of the

constituent particle being introduced, Eq. (1) is reduced to the normal formula of the discrete dipole method

$$\frac{1}{\alpha_i}\boldsymbol{P}(\boldsymbol{r}_i) = \boldsymbol{E}_0(\boldsymbol{r}_i) + k^2 \sum_{j\neq i}^{N} \mathbf{G}(\boldsymbol{r}_i, \boldsymbol{r}_j)\boldsymbol{P}(\boldsymbol{r}_j) \text{ for } i = 1 \text{ to } N. \quad (2)$$

The effective polarizability α_i for the i–th constituent particle is defined by

$$\frac{1}{\alpha_i} = \frac{1}{\alpha_i^0} - \frac{2}{a_i^3}[(1 - ika_i)\exp(ika_i) - 1]$$
$$= \frac{1}{\alpha_i^0} - \left(\frac{k^2}{a_i} + \frac{2}{3}ik^3\right) \quad \text{for} \quad ka_i \ll 1, \quad (3)$$

where $\alpha_i^0 = [(m_i^2 - 1)/(m_i^2 + 2)]a_i^3$. The second term of the RHSs in Eq. (3) arises from taking into account the interaction of a constituent particle with itself, which automatically results in the "radiative reaction term" introduced by Draine (1988).

By solving the 3 N simultaneous equations (2) iteratively, the cross sections of extinction, absorption and scattering of dust aggregates are given by

$$C_{\text{ext}} = \frac{4\pi k}{|\boldsymbol{E}_0|^2} \sum_{i=1}^{N} \text{Im}\{\boldsymbol{E}_{0,i} \cdot \boldsymbol{P}_i^*\}, \quad (4)$$

$$C_{\text{abs}} = \frac{4\pi k}{|\boldsymbol{E}_0|^2} \sum_{i=1}^{N} \text{Im}\{\boldsymbol{P}_i \cdot (\alpha_i^0)^{*-1}\boldsymbol{P}_i^*\}, \quad (5)$$

and

$$C_{\text{sca}} = \frac{k^4}{|\boldsymbol{E}_0|^2} \int d\Omega \left|\sum_{i=1}^{N} [\boldsymbol{P}_i - \boldsymbol{n}(\boldsymbol{n} \cdot \boldsymbol{P}_i)]\exp(-ik\boldsymbol{n} \cdot \boldsymbol{r}_i)\right|^2, \quad (6)$$

where $\boldsymbol{E}_{0,i}$ is the incident electric field at the position $\boldsymbol{r}_i$, and $\boldsymbol{n}$ is the unit vector parallel to the scattering direction.

The accuracy of the approximation was estimated by comparing the result for a sphere composed of 136 dipoles located on a cubic lattice with that obtained by Mie theory for a compact sphere with the same total dipole moment. Even if the size parameter of the constituent particle is small enough, the ratio of the cross section calculated by the discrete dipole method to that by Mie theory approaches to a constant not equal to 1, for $|m|x \ll 1$. The constant ratio increases with increasing value of $|m|$. This deviation from Mie theory is explained by the non–uniformity of electric field inside the volume due to the surface granularity as well as by a lesser screening effect than for a compact sphere (Draine 1988). Therefore, when the optical properties of dust aggregates being calculated by replacing each constituent particle by a dipole, we regard this deviation from Mie theory as an effect of the shape and structure on the optical properties of the dust aggregate. We consider the deviation from the constant ratio at the limit of $|m|x \ll 1$ as the systematic deviation, and then the systematic deviation of the calculations by this method is less than 10% under the condition of $|m|x \lesssim 0.6$.

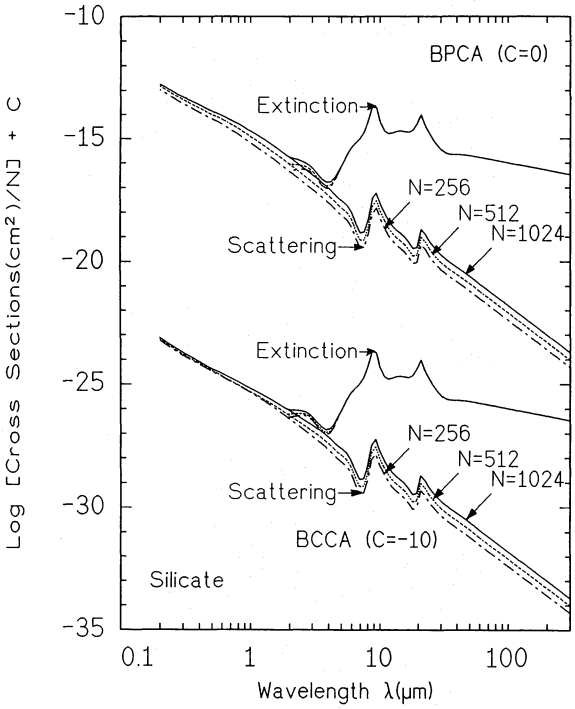

Fig. 2a. The extinction and scattering cross sections per constituent particle of silicate BPCA and BCCA. The dash–dotted, the dashed, and the solid curves denote the dust aggregates whose number of the constituent particles are 256, 512, and 1024, respectively. The curves are shifted by −10 for BCCA

3. Wavelength dependence of the optical properties

We calculated the optical properties of dust aggregates by means of the discrete dipole approximation described in Sect. 2.2. In order to investigate the effect of the differences in sizes and structures on their optical properties, we treat two extreme types of dust aggregates with different numbers of constituent particles shown in Figs. 1a and 1b. We also consider two kinds of minerals as the materials of the constituent particles to investigate the effect of the chemical composition on the optical properties; silicate as an example of dielectric material and magnetite as an absorbing material. The radii of the constituent particles are 0.01 μm. The optical constants used for the calculations are taken from the table of Mukai (1990). The DDA calculations have been performed by modifying the original program coded by Draine & Flatau (see Goodman et al. 1991 for the original code).

The extinction, absorption and scattering cross sections, and the asymmetry parameters of the dust aggregates are obtained by averaging over 12 different configurations by rotating the dust aggregate around three orthogonal incident directions of light. The cross sections and the asymmetry parameter are calculated in wavelengths ranging from 0.2 to 300 μm, where $|m|x \leq 0.6$ for the optical constants used for the calculations, and then the systematic deviation in the calculations is estimated to be less than 10% all over the wavelength as discussed in Sect. 2.2. Also at the same time, we calculated the angular dependence of the degree of linear polarization and of the intensity of the scattered light at the selected wavelengths. The angular dependence of the scattered light will be presented in a forthcoming paper. In this paper the emphasis is put on the wavelength dependence of

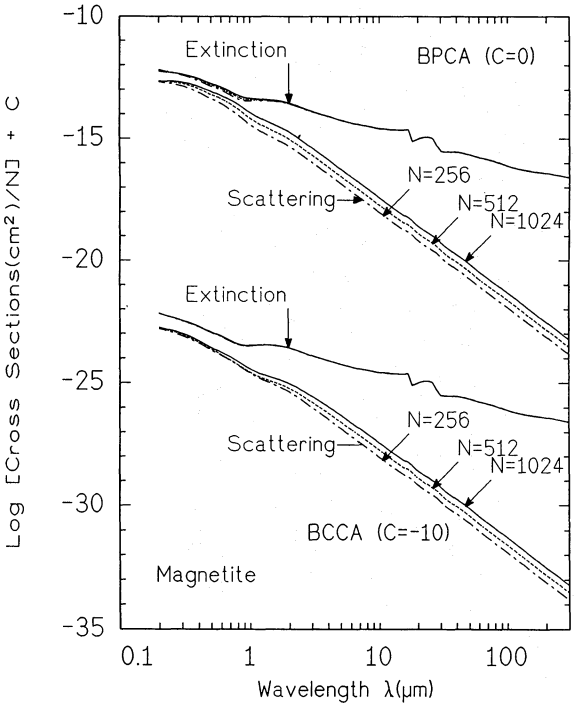

Fig. 2b. The same as Fig. 2a, but for magnetite BPCA and BCCA

extinction, absorption and scattering cross sections, and of the asymmetry parameter.

Figures 2a and 2b show the wavelength dependence of the extinction and scattering cross sections per constituent particle for each type of dust aggregate; Fig. 2a for BPCA and BCCA composed of silicates (referred to as silicate BPCA and silicate BCCA respectively, hereafter) and Fig. 2b for BPCA and BCCA composed of magnetites (referred to as magnetite BPCA and magnetite BCCA).

The extinction cross sections per constituent particle in the region of $\lambda \gg 2\pi a_c$, where the extinction is dominated by the absorption, is independent of the number of the constituent particles (i.e. the size of the dust aggregates) for a given type of dust aggregate. In this region the scattering cross sections per constituent particle vary systematically with the number of the constituent particles regardless of the chemical composition for a given type of dust aggregate. In the following subsections, the behavior of the wavelength dependence of the absorption cross sections, the scattering cross sections and the asymmetry parameter are presented and discussed.

3.1. Absorption cross sections

Figures 3a and 3b show the ratios of the absorption cross sections $C_{abs}(N,\lambda)$ of the dust aggregates consisting of N constituent particles to N times the absorption cross section $C_{abs}(1,\lambda)$ of the constituent particle; Fig. 3a for silicate BPCA and BCCA, and Fig. 3b for magnetite BPCA and BCCA.

In the silicate dust aggregates, around the absorption features at about 10 and 20 μm a ghost effect appears and also a slight enhancement of the ratio $C_{abs}(N,\lambda)/NC_{abs}(1,\lambda)$ is noticeable beyond the 20 μm feature as reported by Bazell & Dwek (1990). The ghost effect around the spectral features is due to the abnormal dispersion across the features, which can be explained in terms of a lesser screening effect due to the change in the values of $|m|$. In the longer wavelength range, the ratio $C_{abs}(N,\lambda)/NC_{abs}(1,\lambda)$ is constant and does not depend on the size and the structure of the dust aggregates. This trend is also true for magnetite BPCA and BCCA, where very slight differences between the dust aggregates exist. We conclude first that in the longer wavelength region the absorption cross section of dust aggregates is proportional to the sum of the cross section of their constituent particles and $C_{abs}(N,\lambda) = \beta N C_{abs}(1,\lambda)$. The proportionality factor β depends on the chemical composition of the constituent particles, but less depends on the structure and on the size of the dust aggregates. It should be kept in mind that the factor β depends on the optical constants used for the calculations; in the present calculations $\beta \sim 1.1$ for the silicate aggregates and ~ 1.35 for the magnetite aggregates.

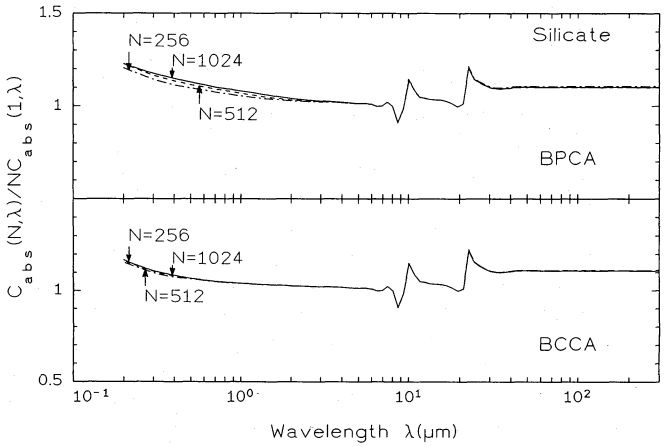

Fig. 3a. The ratios of the absorption cross sections $C_{abs}(N,\lambda)$ of the dust aggregates consisting of N constituent particles to N times the absorption cross section $C_{abs}(1,\lambda)$ of the constituent particle for silicate BPCA and BCCA

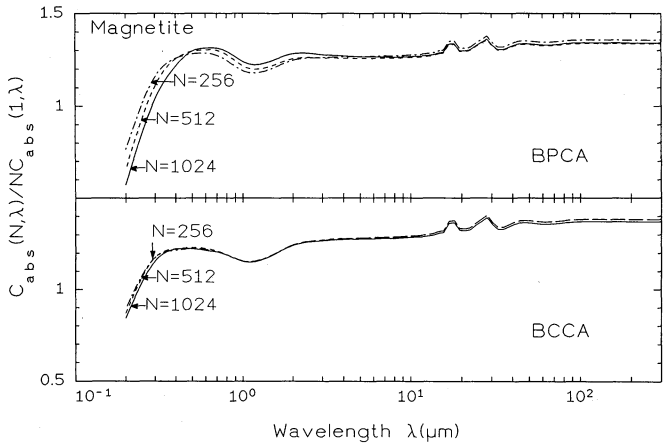

Fig. 3b. The same as Fig. 3a, but for magnetite BPCA and BCCA

It should be noted that the behavior of the absorption cross sections for silicate in the longer wavelength region is different from that by Bazell & Dwek (1990). In their Fig. 4, the ratio of absorption cross section of dust aggregates to that of the mass–equivalent sphere increases gradually from 20 to 80 μm

and then becomes flat (corresponding to $\beta = 2$) beyond 100 μm. Though the optical constants and the dust aggregates used for their calculations are different from ours, our calculations for the "astrophysical silicate" (Draine 1985) show that the ratio is almost constant from 20 to 2000 μm and $\beta \sim 1.2$ for BPCA and BCCA with $N = 256$. Even for amorphous carbon, whose optical constants are taken from the table of Mathis & Whiffen (1989), $\beta \sim 1.3$. The results of our calculations do not show the large enhancement of the absorption efficiency of the dust aggregates in the FIR region in comparison with a compact sphere of the same mass, different from Bazell & Dwek (1990). We have no explanation for the difference, because our method of the calculations is basically the same as the method by Bazell & Dwek (1991), except for the treatment of dust aggregates as described in Sect. 2.2. Recently, Claro & Fuchs (1991) have suggested that higher–order multipole interactions should be taken into account when the ratio of the distance between dipoles to the size of a dipole is less than 1.2. This effect would be important for metallic aggregates and should be investigated in relation to the large enhancement of absorption cross sections in FIR region.

At shorter wavelengths, for silicate aggregates, the ratio $C_{\rm abs}(N,\lambda)/NC_{\rm abs}(1,\lambda)$ is almost constant and independent of wavelength, though there is some variation in the ratio according to the difference in the structure and the size of dust aggregates. On the other hand, for magnetite aggregates, the deviation from the constant ratio becomes prominent towards shorter wavelengths in comparison with silicate aggregates. In magnetite BPCA, the deviation from the constant ratio becomes systematically larger with increasing number of the constituent particles. Magnetite is an absorbing material in comparison with silicate, and BPCA is more compact in structure than BCCA, so that we can deduce that the wavelength dependence of the deviation from the constant values are closely related to the optical thickness of the dust aggregates. This interpretation is discussed and demonstrated in Sect. 4. Here we conclude that the absorption cross section is proportional to the sum of the cross sections of the individual constituent particles when the dust aggregate itself is optically thin.

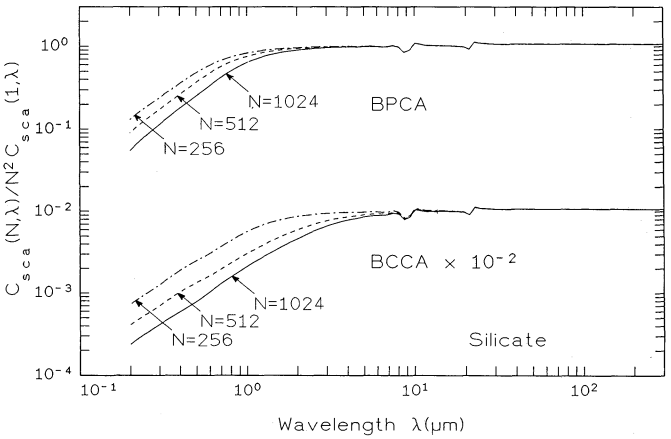

Fig. 4a. The ratios of the scattering cross sections $C_{\rm sca}(N,\lambda)$ of dust aggregates consisting of N constituent particles to N^2 times the scattering cross section $C_{\rm sca}(1,\lambda)$ of the constituent particle for silicate BPCA and BCCA. Note that the values for BCCA are divided by 100

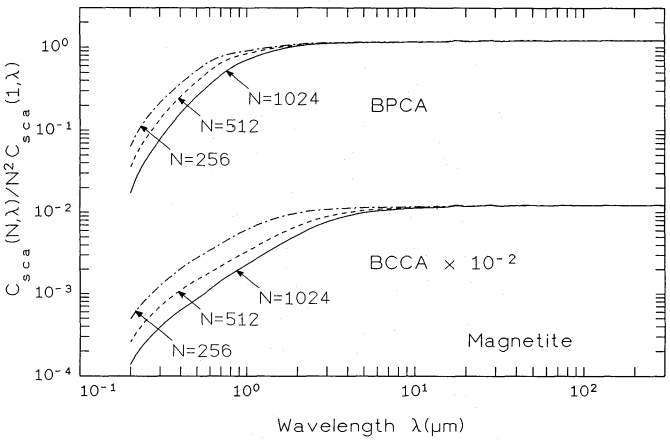

Fig. 4b. The same as Fig. 4a, but for magnetite BPCA and BCCA

3.2. *Scattering cross sections*

The ratio of the scattering cross sections $C_{\rm sca}(N,\lambda)$ of the dust aggregates consisting of N constituent particles to N^2 times the scattering cross section $C_{\rm sca}(1,\lambda)$ of the constituent particle are shown in Fig. 4a for silicate BPCA and BCCA and in Fig. 4b for magnetite BPCA and BCCA.

The ratios are constant in the region of $\lambda \gg 2\pi a_{\rm c}$ and $C_{\rm sca}(N,\lambda) = \alpha N^2 C_{\rm sca}(1,\lambda)$ regardless of the structure and the size of the dust aggregates. The proportionality factor α depends on the chemical composition of the constituent particles, and resultingly depends on the optical constants used for the calculations; for the optical constants used in these calculations, $\alpha \sim 1.1$ for the silicate aggregates and ~ 1.2 for the magnetite aggregates.

The ratio $C_{\rm sca}(N,\lambda)/N^2C_{\rm sca}(1,\lambda)$ deviates from the constant values prominently in the region $\lambda \ll 2\pi a_{\rm c}$ and depends on the size and the structure of the dust aggregates, and on the chemical composition of the constituent particles. However, the behavior of the deviation from the constant ratio towards shorter wavelengths is very similar for a given type of dust aggregate with the same number of constituent particles, regardless of the chemical composition of the constituent particles. When the wavelength dependence of the deviation from the constant ratio is fitted by a function $\alpha[1-\exp(-\lambda_{\rm c}/\lambda)]$, the characteristic wavelength $\lambda_{\rm c}$ is approximately given by $\lambda_{\rm c} = 2\pi a_{\rm c}$. Thus, the wavelength dependence of this ratio is a diagnostic for the size of the dust aggregates, irrespective of the chemical composition of the constituent particles. The measurement of the scattering cross sections at different wavelengths is a useful method to size dust aggregates. Now we can confirm that the characteristic radius $a_{\rm c}$ introduced in Sect. 2.1 represents the size of the dust aggregates.

The size dependence of the scattering cross sections in the region of $\lambda \gg \lambda_{\rm c}$ is simply interpreted as the result of single scattering with coherent scattered light (Berry & Percival 1986). Furthermore, in connection with the behavior of the absorption cross section in the region of $\lambda \gg \lambda_{\rm c}$, the relations $C_{\rm abs}(N,\lambda) \propto NC_{\rm abs}(1,\lambda)$ and $C_{\rm sca}(N,\lambda) \propto N^2 C_{\rm sca}(1,\lambda)$ imply that the optical properties of dust aggregates in this region can qualitatively be described by the Rayleigh approximation. In this region the wavelength dependence of the cross sections of light interaction is qualitatively the same as that of a compact sphere of a mass–equivalent radius $a_{\rm m} = a_0 N^{1/3}$ and is almost independent of the structures of the dust aggregates. The enhancement

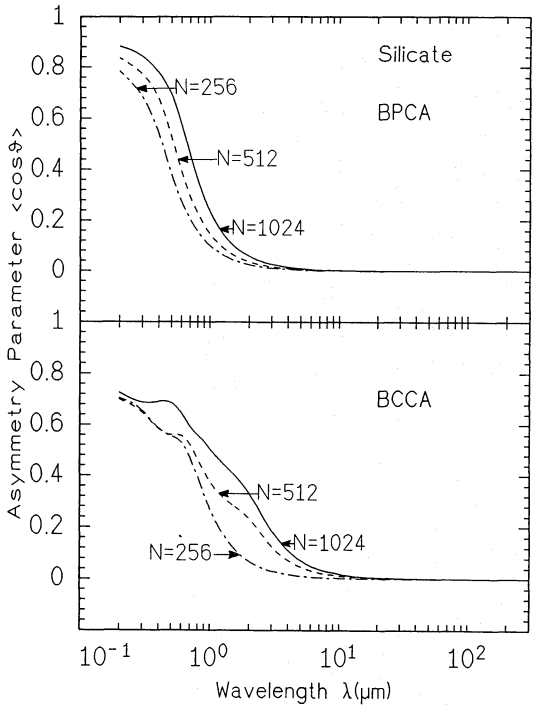

Fig. 5. The wavelength dependence of the asymmetry parameter for silicate BPCA and BCCA. The behavior of magnetite aggregates is quantitatively the same as those of the silicate aggregates

of the absorption and scattering cross sections from the Rayleigh approximation reflects the effect of the aggregation, and depends on the chemical composition of the constituent particles.

3.3. Asymmetry parameter

The wavelength dependence of the asymmetry parameter g is shown in Fig. 5 for silicate BPCA and BCCA. In the region of $\lambda \gg \lambda_c$, the scattering is isotropic, i.e. $g =< cos\theta >= 0$ (strictly speaking, symmetric around the scattering angle 90°). The deviation from the isotropic scattering becomes prominent at about $\lambda = \lambda_c$ according to the characteristic size a_c of the dust aggregates. For BPCA, the asymmetry parameter increases steeply towards shorter wavelengths, while the parameter g gradually increases for BCCA. The parameter g increases with increasing number of constituent particles for each dust aggregate at a given wavelength. The wavelength dependence of the asymmetry parameters for magnetite BPCA and BCCA is quantitatively the same as for silicate BPCA and BCCA, respectively.

For a compact sphere, the forward scattering becomes dominant as the size parameter increases. On the other hand, in spite of the larger size of BCCA, the forward scattering is more prominent at shorter wavelengths for BPCA than for BCCA with the same number of constituent particles. As shown in Figs. 1a and 1b, the dust aggregates used for the calculations are irregularly shaped and are non-homogeneous in structure, being far from a compact sphere in the shapes and in the structures. Thus, the results of the calculations suggest that the wavelength dependence of the asymmetry parameter is also closely related with the structure of the dust aggregates. For BPCA, the scatterers (i.e. constituent particles) are distributed more or less uniformly all over the volume with some concentration towards the center. However, for BCCA, the scatterers are inhomogeneously distributed throughout the volume. The forward scattered light is expected to become more incoherent for BCCA with the dispersed concentration of scatterers than for BPCA. Consequently, the wavelength dependence of the asymmetry parameter reflects not only the size but also the structure of the dust aggregates, independent of the chemical composition of the constituent particles.

4. Discussions

4.1. Optical thickness and absorption cross section of dust aggregates

As pointed out in Sect. 3.1, the wavelength dependence of the absorption cross section seems to depend on the optical thickness of the dust aggregate itself. Here we will derive an empirical formula to reproduce the behavior of the wavelength dependence of the absorption cross section by taking into account the mean optical thickness of the dust aggregate. Although this subject has been discussed by Greenberg & Hage (1990), the problem is how we should estimate the mean optical thickness of dust aggregates.

Generally, when the dust aggregate is represented by a sphere of radius a, the mean optical thickness $\tau_d(N,\lambda)$ of the dust aggregate consisting of N constituent particles is evaluated by

$$\tau_d(N,\lambda) = \frac{4}{3}a \times \frac{3N}{4\pi a^3} C_{ext}(a_0,\lambda), \tag{7}$$

where a_0 is the radius and $C_{ext}(a_0,\lambda)$ is the extinction cross section of the constituent particle. The first term in the RHS of Eq. (7) denotes the mean path length for a sphere with radius a. The problem is reduced to what value we should adopt for the representative radius a of the dust aggregate in evaluating the mean optical thickness. As discussed in Sect. 2.1 and confirmed in Sect. 3.2, the characteristic radius a_c is the most plausible size to represent the size of dust aggregates and to obtain the volume–mean values. However, when we consider the absorption of light in dust aggregates, we should adopt the surface area–equivalent radius a_s as the representative radius of the dust aggregate: The reason is that for dust aggregates composed of absorbing materials, the incident light is completely blocked by the constituent particles directly illuminated and cannot penetrate into the inside. The absorption cross section tends to the geometric cross section, apart from the reduction due to the reflected light. On the other hand, in dust aggregates composed of weakly absorbing materials, the light scattered by a constituent particle interacts with another particle in a dense medium (multiple scattering). This suggests that we should use the absorption cross section $C_{abs}(a_0,\lambda)$ instead of the extinction cross section $C_{ext}(a_0,\lambda)$ in Eq. (7). We define the mean optical thickness of dust aggregates in connection with the absorption cross sections by

$$\tau_d(N,\lambda) = N\left(\frac{a_0}{a_s}\right)^2 Q_{abs}(a_0,\lambda), \tag{8}$$

where $Q_{abs}(a_0,\lambda)$ is the absorption efficiency factor of the constituent particle. Then the absorption cross section of the dust aggregate is approximated with the equation

$$C_{abs}(N,\lambda) = \beta\pi a_s^2\{1-\exp[-\tau_d(N,\lambda)]\} \tag{9}$$

The prefactor β is the constant derived in Sect. 3.1. Equation (9) also reproduces the behavior of the absorption cross sections in

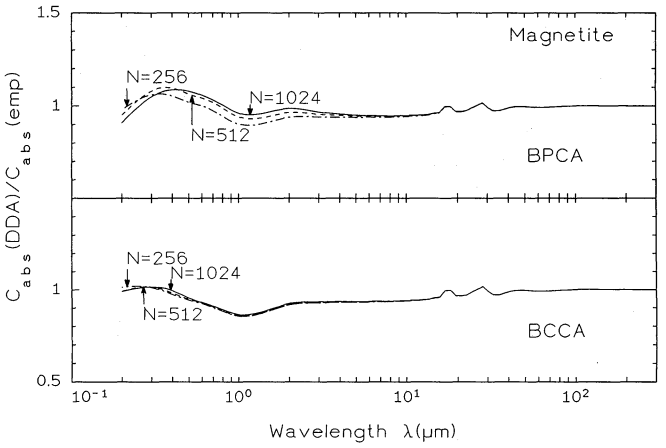

Fig. 6. The ratios of the absorption cross sections calculated by DDA to those evaluated by the empirical formula Eq. (9) for magnetite BPCA and BCCA

the region of $\lambda \gg \lambda_c$, i.e. $C_{abs}(N,\lambda) = \beta N C_{abs}(1,\lambda)$ for $\tau_d(N,\lambda) \ll 1$.

Figure 6 shows the ratios of the absorption cross sections calculated by DDA to those evaluated by the empirical formula Eq. (9) for the magnetite BPCA and BCCA. The empirical formula reproduces the behavior of the wavelength dependence of the absorption cross sections of the dust aggregates within relative error less than 15% all over the wavelengths investigated here, regardless of the structure of the dust aggregates. It should be noted that if we used the characteristic radius a_c instead of a_s in Eqs. (8) and (9), the difference between DDA and the empirical formula is substantially larger in BCCA aggregates. Now we conclude confirmatively that the behavior of the wavelength dependence of the absorption cross sections is related to the optical thickness of the dust aggregates. The absorption cross section is proportional to the sum of the absorption cross section of the constituent particles when the dust aggregate is optically thin. The absorption cross sections can be well reproduced by a simple formula by taking into account the optical thickness of the dust aggregates.

The definition of the mean optical thickness of dust aggregates leads us to the more general discussion on the wavelength dependence of the absorption cross sections of fractal aggregates. In the limit of large sizes, the geometric cross section is proportional to N^γ; $\gamma \sim \frac{2}{3}$ for BPCA and ~ 1 for BCCA. Also γ is ~ 1 for dust aggregates with $D \leq 2$ and is approximately related with the fractal dimension by $D\gamma \sim 2$ for dust aggregates with $2 < D \leq 3$. Then Eq. (8) is reduced to

$$\begin{aligned} \tau_d(N,\lambda) &= \delta N^{(D-2)/D} Q_{abs}(a_0,\lambda) \quad \text{for } 2 < D \leq 3 \\ &= \delta Q_{abs}(a_0,\lambda) \qquad\qquad \text{for } D \leq 2, \end{aligned} \tag{10}$$

where δ is a numerical factor closely related with the formation process of the aggregates and a function of the fractal dimension and the porosity of the dust aggregates (Blum & Kozasa 1992). From Eq. (10), we can see that the optical depth increases for dust aggregates with $D > 2$ as the number of constituent particles increases. The optical depth of dust aggregates with $D \leq 2$ does not depend on the number of constituent particles. Thus the dependence of the absorption cross section on the size is related with the structure of the dust aggregates through the fractal dimension as well as through the porosity.

From Eqs. (9) and (10), we can infer qualitatively the behavior of the size dependence of the temperature of dust aggregates; the temperature of dust aggregates with $D \leq 2$ is almost the same as that of the individual grains, while for dust aggregates with $D > 2$ the temperature varies with the size according to the change in the absorption cross section.

When dust aggregates being in optically thin environments, the temperature T_{gr} of the dust aggregates consisting of N constituent particles is determined by the equation

$$\int_0^\infty C_{abs}(N,\lambda) F_\lambda d\lambda = 4 \int_0^\infty C_{abs}(N,\lambda) \pi B_\lambda(T_{gr}) d\lambda, \tag{11}$$

where F_λ is the radiation flux in the environment and $B_\lambda(T)$ is the Planck function. Note that the prefactor β in Eq. (9) is irrelevant in determining the temperature of dust aggregates in optically thin environments. Figure 7, as an example, shows the dependence of the temperature on the size and the structure of magnetite dust aggregates located at 1 AU from the Sun. In the calculation the radii of the constituent particles are 0.01 μm and the numerical values necessary for the calculations are represented by the values of the dust aggregates with $N = 16384$.

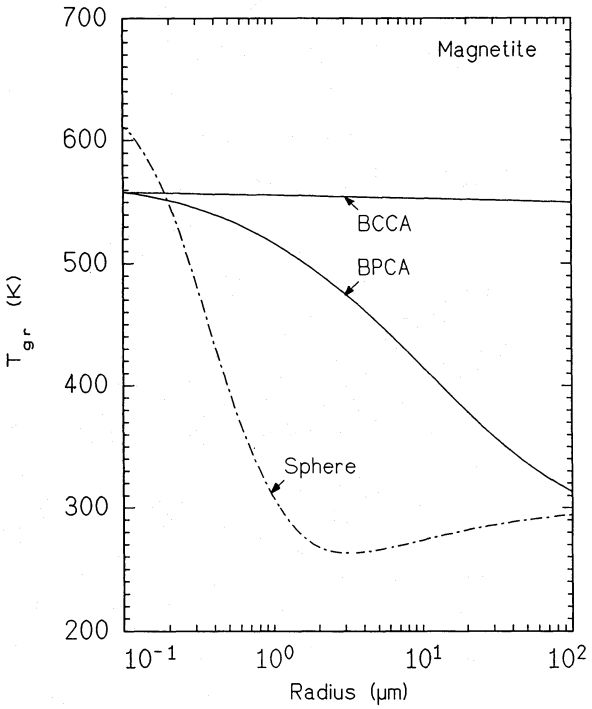

Fig. 7. The size dependence of the temperature of the magnetite BPCA and BCCA located at 1 AU from the Sun. The dash–dotted curve denotes the temperature of compact magnetite sphere calculated by Mie theory. The temperature of the single constituent particle is 568 K

The temperature of the single constituent particle is 568K. As expected, the temperature of the BCCA aggregates is almost constant, independent of their size. The temperature of the BPCA aggregates gradually decreases with increasing size and tends to a constant value when the characteristic radius of the dust aggregates ≥ 100 μm. On the other hand, the compact magnetite sphere approaches steeply to the black body temperature around a radius of ≥ 10 μm. The dependence of the temperature on the size and the structure of the dust aggregates plays a crucial role

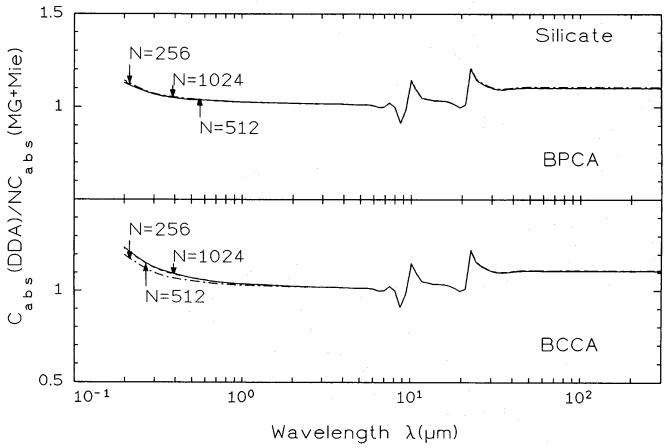

Fig. 8a. The ratios of the absorption cross sections calculated by DDA to those by the MG+Mie theory for silicate BPCA and BCCA

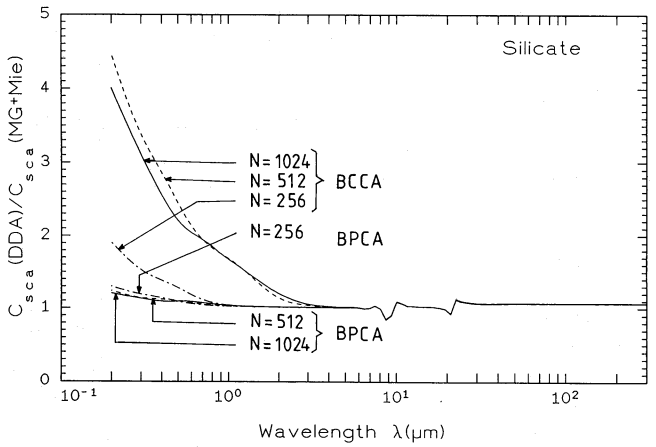

Fig. 8b. The same as Fig. 8a, but for the scattering cross sections

in considering the physical and chemical evolution of dust grains in interplanetary as well as in interstellar space.

4.2. The validity of the application of the effective medium theory

The effective medium theory would be an efficient method to evaluate the optical properties of dust grains with porous and fluffy structures if the theory were applicable. Two popular methods have been applied to investigate the optical properties of dust in space; the Maxwell–Garnett mixing rule and the Bruggeman mixing rule (Jones 1988; Mathis & Whiffen 1989; Greenberg & Hage 1990; Mukai et al. 1992). The validity of the application to dust grains with fluffy structure as well as with rough surfaces has been discussed in comparison with the DDA calculations (Perrin & Lamy 1990; Perrin & Savin 1990; Hage & Greenberg 1990; Bazell & Dwek 1990). However, the comparison has been limited to dust grains with a particular and/or artificial structure. The application of the mixing rules is questionable for dust aggregates with non–homogeneous structures (Bohren & Huffman 1983). Here we investigate the applicability of the effective medium theory for dust aggregates by comparing with the results of our DDA calculations.

We apply the Maxwell–Garnett mixing rule to the dust aggregates by regarding the constituent particles as inclusions embedded in vacuum and calculate the cross sections by Mie theory (hereafter referred to as the MG + Mie theory for convenience). The average dielectric function ϵ_{av} is given by

$$\epsilon_{av} = 1 + 3f\frac{\epsilon - 1}{(\epsilon + 2) - f(\epsilon - 1)}, \tag{12}$$

where ϵ is the dielectric function of the constituent particles and the mean concentration f of the constituent particles is related with the mean porosity of dust aggregates by $f = 1 - P$. The absorption, scattering and radiation pressure cross sections are calculated for a sphere of characteristic radius a_c and an average dielectric function ϵ_{av} by Mie theory. In this paper the comparison is confined to silicate BPCA and BCCA.

Figures 8a to 8c show the ratios of the cross sections calculated by DDA to those by the MG+Mie theory for silicate BPCA and BCCA; Fig. 8a for the absorption cross sections, Fig. 8b for the scattering cross sections and Fig. 8c for the radiation pressure cross sections. Note the difference in the scales between the figures.

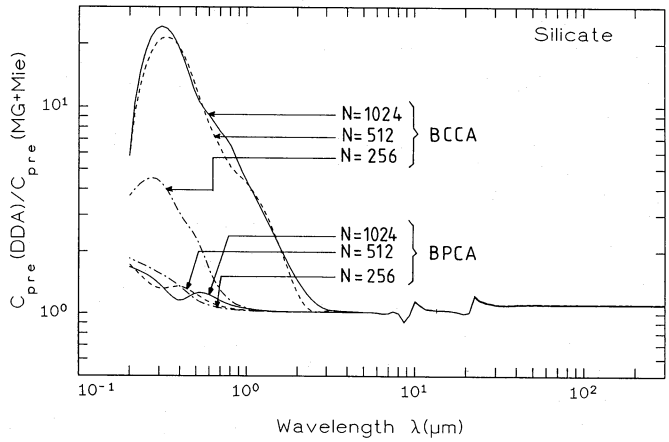

Fig. 8c. The same as Fig. 8a, but for the radiation pressure cross sections

The wavelength dependence of the absorption cross sections can be well reproduced by the MG+Mie theory, regardless of the aggregate structures and sizes. The ratio $C_{abs}(\mathrm{DDA})/C_{abs}(\mathrm{MG+Mie})$ is almost constant all over the wavelength region, and the trend is almost the same as those in Fig. 3a. This is understood by the fact that the absorption cross section is proportional to $\mathrm{Im}\{\alpha\}$ (α is the polarizability of the sphere) if $|m-1|x \ll 1$. The result is insensitive to how the porosity is defined if the porosity is high enough, as far as the polarizability is the same as that of the dust aggregates. This fact also suggests that when the dust aggregates themselves are optically thick, the MG+Mie theory will be sensitive to the definition of the mean porosity and will fail to reproduce the wavelength dependence of the absorption cross section.

The scattering and radiation pressure cross sections are reasonably reproduced by the MG+Mie theory for BPCA, although the difference is significant at shorter wavelengths. On the other hand, both cross sections for BCCA cannot be reproduced in the region of $\lambda \ll \lambda_c$, where the scattering cross sections heavily depend on the structure as well as on the size of the dust aggregates as shown in Sect. 3.2. It should be noted that the radiation pressure cross sections for magnetite BPCA and BCCA are reasonably reproduced by the MG+Mie theory, because the cross section is dominated by the absorption for absorbing materials.

Resultingly, the MG+Mie theory is an efficient method to obtain the optical properties of dust aggregates whose constituent particles are uniformly distributed all over the bodies such as BPCA when the dust aggregates are optically thin. The theory fails to reproduce the optical properties in the region of $\lambda \ll \lambda_c$ for dust aggregates with very fluffy and non–homogeneous structures such as BCCA, except for the absorption cross section.

5. Concluding remarks

The discrete dipole approximation, by replacing each constituent particle by a dipole, has been applied to two types of dust aggregates with different numbers and chemical compositions of the constituent particles, in order to investigate the effects of structure, size and chemical composition on the optical properties of the dust aggregates. Although our calculations are limited to somewhat small dust aggregates (< 0.2 μm for BPCA and < 0.52 μm for BCCA) due to the capability of the computers we could access, we derived the following results:

(1) In the region $\lambda \gg \lambda_c$, the dust aggregates behave as dipoles. The wavelength dependence of the optical properties of dust aggregates is qualitatively reproduced by the Rayleigh approximation for a compact sphere with the same mass, and does not depend on their structure.

(2) The behavior of the scattering cross sections around $\lambda = \lambda_c$ is a diagnostic for the size of dust aggregates, regardless of the chemical composition.

(3) The wavelength dependence of the absorption cross sections is explained in terms of the optical thickness of the dust aggregates, and is reasonably reproduced by a simple formula. This formula could also be applicable for dust aggregates composed of constituent particles with sizes and chemical compositions different from the dust aggregates presented here.

(4) The wavelength dependence of the asymmetry parameter reflects the size as well as the structure of the dust aggregates. BPCA are characterized by a prominent forward scattering in the region of $\lambda \ll \lambda_c$, in spite of their smaller size in comparison with BCCA with the same number of constituent particles.

(5)The Maxwell–Garnett mixing rule is applicable for dust aggregates with uniform structures such as BPCA, but not for dust aggregates with non–homogeneous structures such as BCCA except for the absorption cross sections.

In this paper, the emphasis was put on the wavelength dependence of the optical properties. The angular dependence of the scattered light can be useful to reveal the nature of dust aggregates, which will be presented in a forthcoming paper. When we consider applications to dust aggregates in space, we must extend the calculations to dust aggregates composed of several kinds of minerals, and of core–mantle type grains. The variations of spectral features could be a diagnostic to investigate the aggregation process in space. Also the size distribution of the constituent particles is a key factor to clarify the nature of the dust grains in space. These subjects are left for the future investigations.

Acknowledgements. The authors thank Dr. B. T. Draine for providing us the original program of the discrete dipole approximation. T. K. is grateful to Profs. H. Fechtig and H. J. Völk for their hospitality during his stay at the Max–Planck–Institut für Kernphysik. J. B. is supported by the Deutsche Forschungsgemeinshaft under grant Ig 3/13–4. T. M. acknowledges the support from the Scientific Research Fund of the Ministry of Education, Science, and Culture (02640205). The numerical calculations have been performed by using Vax–Stations 3100, 3600 and 8650 at MPI–K.

References

Bazell, D., Dwek, E., 1990, ApJ 360, 142
Berry, M. V., Percival, I. C., 1986, Optica Acta 33, 577
Blum, J., Kozasa, T., 1992, in preparation
Bohren, C. F., Huffman, D. R., 1983, Absorption and Scattering of Light by Small particles, John Wiley & Sons, New York
Brownlee, D. E., Tomandl, D. A., Hodge, P. W., 1976, In: Elsässer, H., Fechtig, H (eds.) IAU. Colloq. 31, Interplanetary Dust and Zodiacal Light, Springer–Verlag, Berlin, p. 279
Claro, F., Fuchs, R., 1991, Phys. Rev. B 44, 4109
Draine, B. T., 1985, ApJS 57, 587
Draine, B. T., 1988, ApJ 333, 848
Giese, R. H., Weiss, K., Zerull, R. H., Ono, T., 1978, A&A 65, 265
Greenberg, J. M., Hage, J. I., 1990, ApJ 361, 260
Goodman, J. J., Draine, B. T., Flatau, P. J., 1991, Optics Letters 16, 1198
Hage, J. I., Greenberg, J. M., 1990, ApJ 361, 251
Jones, A. P., 1988, MNRAS 234, 209
Mathis, J. S., Whiffen, G., 1989, ApJ 341, 808
Mathis, J. S., 1990, ARA&A 28, 37
Muinonen, K., Lumme, K., Peltoniemi, J., Irvine, W. N., 1989, Appl. Opt. 28, 305
Mukai, T., 1990, In: Bonetti, A., Greenberg, J. M., Aliello, S. (eds.) Evolution of Interstellar Dust and Related Topics, Elsevier, Publishers B. V., North–Holland, p. 397
Mukai, T., Ishimoto, H., Kozasa, T., Blum, J., Greenberg, J. M., 1992, in press
Ossenkopf, V., 1991, A&A 251, 210
Perrin, J. M., Lamy, P. L., 1990, ApJ 364, 146
Perrin, J. M., Sivan, J. P., 1990, A&A 228, 238
Perrin, J. M., Sivan, J. P., 1991, A&A 247, 497
Purcell, E. M., Pennypacker, C. R., 1973, ApJ 186, 705
Wright, E. L., 1987, ApJ 320, 818

This article was processed by the author using Springer-Verlag TEX A&A macro package 1991.